Trop J Nat Prod Res, November 2024; 8(11): 9296 - 9309 **ISSN 2616-0684 (Print)**
ISSN 2616-0692 (Electronic)

Tropical Journal of Natural Product Research

Available online at https://www.tjnpr.org

Original Research Article

Green synthesis of Characterized Bio-functionalized ZnO Nanoparticles from *Terminalia catappa* (Almond) Methanol Leaf Extract and their Potential Antioxidant and Antibacterial Properties

Johnson O. Momoh[1]*, Sanjeev Kumar[2], Oluremi N. Olaleye[3], Oluwasegun M. Adekunle[1] and Taiwo S. Aiyelero[1]

[1]*Department of Chemical Sciences, College of Basic Science, Lagos State University of Science and Technology (LASUSTECH), Ikorodu, Lagos State, Nigeria.*
[2]*Department of Physics, Chandigarh University, Gharuan Mohali-140413, India.*
[3]*Department of Biological Sciences, College of Basic Science, Lagos State University of Science and Technology (LASUSTECH), Ikorodu, Lagos State, Nigeria.*

ARTICLE INFO

Article history:
Received 29 January 2024
Revised 01 October 2024
Accepted 24 October 2024
Published online 01 November 2024

ABSTRACT

Synthesis of zinc oxide nanoparticles (ZnO-NPs) using plants has been suggested to have biological applications. ZnO-NPs were synthesized using *Terminalia catappa* (Almond) methanol leaf extract and $Zn(CH3COO)_2.6H2O$ as precursors. UV-visible spectroscopy (UV-vis), X-ray diffraction (XRD), scanning electron microscopy–energy-dispersive X-ray spectroscopy (SEM-EDX), and Fourier transform infrared (FTIR) were used to characterize the ZnO-nanoparticles. The antioxidant, GC-MS, and antibacterial activities were determined using standard methods. The phytochemical screening of the extract shows that it contains alkaloids, flavonoids, tannins, saponins, etc. The GC-MS analysis of the Almond extract indicated the presence of 12 different compounds, with the 9, 17-Octadecadienal-Z being the most abundant. The UV–vis analysis has absorption peaks at 370 nm; SEM shows a quasi-spherical-like shape, while EDX indicates that the ZnO-NPs contain oxygen (54.93%) and zinc (36.14%). The optical energy band gap of 3.353 eV was obtained. The average crystallite size of the ZnO-NPs was 53.46 nm with a dislocation density of 0.000349899 $(nm)^{-2}$. FTIR spectrum revealed the presence of organic moieties serving as reducing and capping agents. The extract and the ZnO-NPs have antioxidant scavenging activity. The extract and tetracycline exhibited a moderate and strong antibacterial response against *Klebsiella pneumonia*, *Salmonella typhi*, *Pseudomonas aeruginosa, Escherichia coli, and Staphylococcus aureus,* while the nanoparticles exhibited a weak and moderate response. The MIC and MBC values of the extract against the bacteria strains ranged from 12.50 to 25, and 25 to 50 mg/mL, respectively. The study supports the plant's traditional uses for treating infections and other diseases.

Keywords: *Terminalia catappa*, phytochemical analysis; nanoparticles, antioxidant and antibacterial activity.

Introduction

Recent advances in science have given rise to the area of nanotechnology, which studies the physical, biological, chemical, and engineering sciences at the nanoscale.[1] Because of their extremely small sizes between 1 and 100 nm and high surface-to-volume ratio, which leads to an increase in both physical and chemical variations in their properties such as catalytic properties, melting points, mechanical properties, biological and sterical properties, thermal and electrical conductivity, and optical absorption—nanoparticle research has attracted a lot of attention.[2] Because of its adjustable and versatile morphological, photonic, and spintronic characteristics, zinc oxide (ZnO) is one of the most researched n-type semi-conducting metal oxide materials.[3,4] It is distinguished by a high excitation energy of 60 meV and a broad direct band gap energy of 3.37 eV.[5] These properties have numerous functions, like high room temperature luminescence, good transparency, electron mobility, etc.

*Corresponding author. Email: momohjohnson2008@gmail.com
Tel : +234 8056374756

Citation: Momoh JO, Kumar S, Olaleye ON, Adekunle OM, Aiyelero TS. Green synthesis of Characterized Bio-functionalized ZnO Nanoparticles from *Terminalia catappa* (Almond) Methanol Leaf Extract and their Potential Antioxidant and Antibacterial Properties. Trop J Nat Prod Res. 2024; 8(11): 9296 – 9309. https://doi.org/10.26538/tjnpr/v8i11.46

Official Journal of Natural Product Research Group, Faculty of Pharmacy, University of Benin, Benin City, Nigeria

These properties are used in applications such as catalysts,[6] photocatalysts,[7-9] antibacterial studies,[10] anti-biofilm,[11] and anti-diabetic activities,[12] photodetectors,[13] solar cells,[14] drug delivery, and nanomedicine.[15,16]

ZnO-NPs can be generated using numerous processes, such as pulsed laser deposition,[17] hydrothermal,[18] solvothermal[19], and the sol-gel method.[20] Some of these methods are generally labour-intensive, harmful to living organisms and our environment, and expensive.[21] The creation of environmentally friendly nanoparticles without the use of toxic materials has garnered research attention in recent years.[22] Green materials can function as both stabilizing and reducing agents for the synthesis of different metal oxide nanoparticles.[23,24] This biological approach looks to be a more affordable option than traditional physical and chemical methods of nanoparticle synthesis. Plant leaf extract,[25,26] enzymes,[27] and bacteria,[28] play crucial functions in the production of nanoparticles. The major sources of foodborne diseases in humans are caused by the consumption of food materials contaminated with foodborne organisms such as fungi, bacteria, and viruses. Some common bacteria found in food substances are *Escherichia coli*, *Klebsiella pneumonia*, *Staphylococcus aureus*, *Salmonella typhi*, and *Bacillus spp.*[29,30] The control of foodborne diseases is an important aspect of public health.[29] The incidence of antibiotic resistance in these microorganisms has limited the use of different antibiotics and other currently used methods to control these diseases. This has resulted in the emergence of highly resistant bacteria that are resistant to most antibiotics.[29] Most of these microorganisms' antibiotic resistance mechanisms are irrelevant for most nanoparticles because their

biochemical mode of action involves making direct contact with the bacterial cell wall rather than entering the cell.

Medicinal plants used in traditional medicine in most countries of the world are the major sources of phytochemicals that impede the growth of microorganisms causing infectious diseases. This has made researchers focus on plant-derived compounds as possible bioactive agents against infectious diseases. Numerous studies have shown that different medicinal plants have antimicrobial activities,[31-33] antimalarial potentials, [34-35] hepatoprotective effects, [36-38] antidiabetic activities, [39-41] and inhibition of *in vitro* glycation product production.[42]

Terminalia catappa L. is a naturally occurring tropical plant in the Combretaceae family. It is native to Malaysia and found in the West (countries like Nigeria) and Central Africa. Numerous studies have shown that *T. catappa* has aphrodisiac effects, antiviral, antimicrobial, anti-diabetic, anti-inflammatory, anti-cancer, antioxidant, immunogenicity, dietary, and hepatoprotective activities.[43-45] This study aimed to produce ZnO-NPs utilising methanol leaf extract of *Terminalia catappa* and evaluate its antioxidant and antibacterial activities as well as the plant extract against four Gram-negative bacteria strains (*Salmonella typhi, Klebsiella pneumonia, Pseudomonas aeruginosa,* and *Escherichia coli*) and one Gram-positive bacteria strain (*Staphylococcus aureus*).

Materials and Methods

Chemicals and materials

Sodium hydroxide (NaOH: ≥ 98% purity), zinc ethanoate hexahydrate ($Zn(CH_3COO)_2.6H_2O$:≥ 98% purity), methanol (CH_3OH:≥99.9% purity), DPPH (2, 2 Diphenyl-1-picrylhydrazyl:≥99.9% purity), potassium ferricyanide ($K_3[Fe(CN)_6]$:≥99.9% purity), trichloroacetic acid (CCl_3COOH : ≥ 98% purity), and ferric chloride ($FeCl_3$: ≥ 98% purity) are analytical grade reagents used in this research, were sourced from Sigma-Aldrich (St. Louis, Missouri, United States of America (USA). Nutrient agar, nutrient broths, and deionized water (DW) were also used in this study.

Collection and identification of plant material

The leaf of *T. catappa* was obtained from LASUSTECH Ikorodu, Nigeria (latitude: 6° 35' 59.99" N, longitude: 3° 29' 59.99" E). The leaves were identified by Mrs. Oluremilekun Olabisi Sokefun, a botanist from the Department of Biological Sciences, Lagos State University of Science and Technology (LASUSTECH), Ikorodu, Lagos State, Nigeria.

Preparation and extraction of plant material

The leaves of *T. catappa* were cleaned and washed with deionized water and air dried for fourteen days under shade in the Department of Chemical Sciences at LASUSTECH. 200 g of the ground material was soaked with 2 L of 80% methanol at 25 ± 2°C for seventy-two hours with intermittent shaking. The extract was filtered using cotton wool and Whatman No. 1 filter paper and the filtrate was concentrated at a temperature not exceeding 40 °C using a rotary evaporator. The concentrated *T. catappa* extract was then dried for 48 hours at 40 °C in an aerated oven until it was completely dry and then kept at 4 °C in a refrigerator.

Phytochemical analysis of the extract

Phytochemical analyses were performed on the *T. catappa* methanol leaf extract to determine its phytochemical contents using standard protocols.[31, 38, 46]

Screening of phytochemicals found in the plant extract using UV–vis spectrophotometer

The modified method of Theng and Korpenwar,[47] was used for the screening of phytochemicals found in the plant extract using UV-Vis spectrophotometer. Briefly, the plant extract (0.01, 0.02, and 0.03 mg/10 mL) was filtered through Whatmann No. 1 filter paper after centrifuging at 3000 rpm for 10 min. The extract was diluted in a 1:10 ratio with the same solvent (DW). Using a 6850 UV/Vis. Spectrophotometer (JENWAY), the plant extract was examined at wavelengths ranging from 200 to 800 nm, and the distinctive peak values were recorded. The UV-Vis's characteristic peaks were found, and their wavelength values were noted. The wavelength ranges for particular phytochemicals or secondary metabolites were recorded.

GC-MS analysis of the leaf extract

GC-MS analysis of the *T. catappa* extract was examined using an Agilent Technology 7890 GC machine fitted with a mass spectrometric detector using the protocol explained by Momoh *et al*.[35]

Component detection

Interpretation of the mass spectrum: For the GC-MS analysis, more than 62,000 patterns stored in the National Institute Standard and Technique (NIST) database were used for the analysis. The spectra of the known compounds stored in the NIST collection were compared with those of the undetermined compounds found in the extract. The test sample's compounds' names, molecular weights, formulas, and structures were identified.

Biofabrication of ZnO-NPs synthesized from T. catappa extract.

ZnO-NPs were produced with minimal alterations utilizing a modified hydrothermal chemical precipitation procedure as described by Gaur *et al*. (2023).[7] Briefly, a 0.1 M solution of $Zn(CH_3COO)_2.6H_2O$ was prepared by dissolving 2.3 g of the zinc acetate salt in 100 mL in a conical flask. 300 mL of the *T. catappa* methanol extract (3 g in 300 mL DW) solution was mixed with the zinc acetate salt solution; the mixture was stirred, and placed on a magnetic stirrer for 60 min at 60 ºC. The phytochemicals present in the *T. catappa* extract were used as reducing and capping agents. The reaction mixture solution pH was adjusted to 10 by adding sodium hydroxide (0.2 M) drops and cooled down. After 2 h, the colloidal solution became milky, indicating the formation of ZnO-NPs. After that, the solution was placed in a centrifuge and run for 15 min at 2000 rpm. The resulting supernatant was poured off, centrifuged once more, cleaned with DW, and allowed to dry in an oven at 109°C for 2 h. The precipitate was put in a crucible and heated to 450°C for 2 h in a muffle furnace. ZnO-NPs were obtained by crushing and powdering the dried precipitate and stored in an airtight container. The synthesized ZnO-NPs were characterized and the antioxidant, and antibacterial activity were investigated.

Characterization of ZnO-NPs synthesized from T. catappa extract

6850 UV-visible spectrophotometer **(**UV/Vis) Jenway was employed for the spectrometric analysis of ZnO-NPs synthesized from *T. catappa* extract measured periodically at a range of 250–430 nm. A spectrum of ZnO-NPs was plotted with wavelength on the x-axis and absorbance on the y-axis. The absorbance peaks were recorded. The morphology and chemical content of the biosynthesized *T. catappa*/ZnO-NPs were analysed with the Phenom Prox model Scanning Electron Microscopy-Energy-Dispersive X-ray spectroscopy (SEM-EDX) equipment (phenomWorld Eindhoven, Netherlands). The structural properties, like crystallite size, of the prepared ZnO-NPs synthesized from almond extract were investigated via XRD (XRD Empyrean Malvern Panalytical diffractometer).

FTIR analysis

FTIR was used to determine the functional groups of organic compounds. The ZnO-NPs synthesized from *T. catappa* extract were investigated using a Shimadzu FTIR-8400S spectrometer for the presence of phytochemicals.

Antioxidant assay

DPPH assay

The antioxidant activity of the *T. catappa* extract and the ZnO-NPs synthesized from *T. catappa* was carried out by the Siripi *et al*. (2017)[48] method using the DPPH assay to determine the percentage scavenging capacity. In the current study, 1 mL of 50% methanol along with ascorbic acid (standard) and different concentrations of the *T. catappa*/ZnO-NPs (20, 40, 60, 80, and 100 µg/mL) were added separately to 1 mL of 1 mM DPPH in different test tubes and incubated at 37 ºC under dark conditions for 30 min, and then the

absorbance at 517 nm was measured using a UV-visible spectrophotometer. ABS_1 is the absorbance of standard ascorbic acid, while ABS_2 is the absorbance of the extract and the ZnO-NPs.

$$\% \text{ DPPH radical scavenging activity} = \frac{ABS_1 - ABS_2}{ABS_1} \times 100$$

The concentrations of *T. catappa* extract in µg/mL and ZnO nanoparticles in mg/mL needed to scavenge 50% of the DPPH radical were defined as the IC_{50}. Ascorbic acid served as the control.

Ferric-reducing power assay (FRAP)

The FRAP assay was carried out with a minor modification utilizing ascorbic acid as the standard control, as previously reported by Momoh *et al*. (2023).[42] Briefly, separate test tubes were filled with 2.5 mL of deionized water, diluted *T. catappa* extract, and ZnO-NPs (50–300 mg/mL) together with 2.5 mL of $K_3[Fe(CN)_6$ (2.5 mL, 1% w/v) and 2.5 mL of phosphate buffer with a concentration of 0.2 M at pH 6.6. The mixture in the individual test tubes was then mixed with 2.5 mL of 10% w/v CCl_3COOH after it had been incubated at 50 °C for 20 min. This was later centrifugation at 3000 rpm for 10 min. 2.5 ml of deionized water and 0.1 % w/v of $FeCl_3$ solution were combined with 5 mL of the supernatant. A 6850 UV-visible spectrophotometer (JENWAY) was used to measure the absorbance of the resultant solution at 700 nm following 30 min of incubation at room temperature in the dark. The ferric-reducing power capacities of *T. catappa* extract, ZnO-NPs, and the standard control were expressed graphically by plotting the absorbance against concentration. The assays were repeated three times.

Test organisms used for the study.

The antibacterial activity of *T. catappa*/ZnO-NPs and the leaf extract of *T. catappa* against four Gram-negative bacteria strains (*Klebsiella pneumonia, Salmonella typhi, Escherichia coli,* and *Pseudomonas aeruginosa*) and one Gram-positive bacteria strain (*Staphylococcus aureus*) was investigated. The five different bacteria used in this study were maintained at 4 °C on five different nutrient agar slants in the Biochemistry laboratory, and fresh subcultures of these bacteria were made before use.

Inoculum preparation

Test tubes containing a loopful of isolated colonies of each of the five different bacteria were inoculated individually with 4 mL of purified peptone water and incubated for 4 h at 37 °C. Using the standard procedure described by Momoh *et al*.,[32] these bacterial suspensions were then adjusted with peptone water to generate turbidity visually comparable to that of 0.5 McFarland standards. About 1 x 10^8 colony forming units per milliliter (CFU/mL) was the solution's turbidity.[32]

Determination of the zones of inhibition

Antibacterial activities of the synthesized *T. catappa*-mediated ZnO-NPs and the methanol leaf extract of *T. catappa* were performed against all five different bacteria strains. ZnO nanoparticles and *T. catappa* extract were tested for antibacterial activity using the standard procedure of the agar well diffusion method. The five distinct microorganisms were cultured in broth for eighteen hours, with each being suspended in a different sterile nutrient broth. To standardize the broths, 9% normal saline was added, and their turbidity was measured against the McFarland standard. 25 mL of the autoclaved nutritional agar were loaded into Petri dish plates, and the agars were allowed to harden. 100 µL of different standardized cultures (adjusted to 0.5 McFarland) of the five different organisms were added to the different nutrient agar plates. Next, a cork borer was used to punch three wells out of the surface of each plate. To stop nanoparticles from leaking out of the bottom of the 6 mm wells punched into the nutrient agar plates to assess the antibacterial activity of ZnO nanoparticles; one drop of melted agar (0.8% agar) was used to seal the wells.

100 µL (100 and 200 mg/mL of the extract of *T. catappa* and 1 mg/L of *T. catappa* mediated ZnO-NPs) of the nanoparticle suspension and that of the extract solution were poured into each of the three wells on all the plates and allowed to diffuse for 2 h at room temperature. For the antibacterial investigation, the plates were incubated at 37 ºC for 18 to 24 hours. The inhibitory zone's sizes were measured in millimetres. The susceptibility of the five different organisms (*S. aureus, K. pneumonia, S. typhi, E. coli,* and *P. aeruginosa*) to the *T. catappa* mediated ZnO nanoparticle and that of the extract of *T. catappa* was assayed using the modified standard method illustrated by Momoh *et al.*[32] The average values were recorded after the experiment was conducted three times. There were five categories used to categorize the inhibitory responses: little or no response (zone diameter <10 mm); weak response (zone diameter between 10-15 mm); moderate response (zone diameter between 16-20 mm); strong response (zone diameter between 21-30 mm); and potent response (zone diameter > 30 mm). Deionized water served as the negative control. Tetracycline was used as a positive control.

Minimum inhibitory concentration (MIC) of T. catappa extract

The absence of any visible turbidity in the experimental tube when compared to the control tube indicates the MIC of the extract, which stopped the test organisms from growing. The MIC values of the *T. catappa* extract against the five different bacterial strains were determined using the standard method.[32] Serial dilution was used to measure the extract's MIC values against each of the five species. A series of various test tubes were filled with 1 mL of Mueller-Hinton broth and autoclaved. After that, 1 mL of 100% of the *T. catappa* extract solution (2 g/mL) was poured into the first separate test tubes to make a concentration of 50 %, and serial dilutions were carried out on all the test tubes. Overnight broth cultures of the five different Gram-negative and Gram-positive bacteria strains were adjusted to the McFarland turbidity standard, and 100 µL of the various cell suspensions were added to each of the separate test tubes. All the test tubes were incubated in an ovum aerobically at 37 °C for 18 h. A negative control tube was used in the experiment by adding 1 mL of normal saline to all the bacterial strains in separate tubes. The lowest concentrations of the extract solutions without bacterial growth for all the organisms were considered the MIC.

Minimum Bactericidal Concentration (MBC) of T. catappa extract

The *T. catappa* extract's MBC value was performed using standard procedure.[32] 0.1 mL aliquots of test samples from the MIC assay non-turbid tubes were subcultured onto nutrient agar plates. The resultant nutrient agar plates were incubated aerobically for 24 h at 37 °C. The extract solution's lowest concentration at which no colonies of *Klebsiella pneumonia, Salmonella typhi, Staphylococcus aureus, Pseudomonas aeruginosa,* and *Escherichia coli* were taken as the MBC. Sterilized deionized water was used as a negative control tube, and the findings were compared with it. On a set of new agar plates, the concentration of the extract solution that did not exhibit any growth was taken to be the MBC. The MBC is defined as the lowest MIC value that showed no visible growth. The MBC/MIC value was determined to be either bacteriostatic or bactericidal. The MBC/MIC ratio is considered bacteriostatic if its value is greater than 4 and bactericidal if its value is less than or equal to 4.

Statistical analysis

A P value < 0.05 was considered significant. All analyses were conducted in triplicate, and the mean ± SD was used to express the results. The student's t-test was used for comparison. A one-way analysis of variance (ANOVA) post-hoc Turkey test was used to analyze the data using GraphPad Prism computer software version 5.01 (USA).

Results and Discussion

The phytochemical screenings of the leaf extract of *T. catappa* showed that the extract contains secondary metabolites like tannins, flavonoids, alkaloids, phenolic compounds, anthraquinones, triterpenoids, saponins, and reducing sugar, as shown in Table 1. Several studies have shown that *T. catappa* contains secondary metabolites like tannins, gallic tannins, catechin, tannins, glycosides, carbohydrates, and triterpenoids.[49-51] Secondary metabolites like alkaloids, tannins, cardiac and cyanogenic glycosides, steroidal aglycone, and saponins have been associated with the antimicrobial activities of different herbal products.[52] According to a study, the presence of saponins and flavonoids found in garlic plants helps in

the treatment of bacterial and related human diseases used in traditional medicine.[53] It has been documented that phenolic compounds may integrate into Gram-positive bacteria lipid monolayers, perhaps increasing the fluidity of the membrane. Furthermore, phenolic compounds have the potential to disrupt lipoproteins and increase membrane fluidity, which could impact their cellular metabolism and later lead to bacterial cell death.[33] Gill and Holley's study,[54] has shown that antimicrobial compounds found in plant extracts may interact with proteins and enzymes found in the cell membrane of microorganisms, causing it to rupture and leading to the release of protons toward outside the cells, which may destroy enzymatic architecture or prevent the production of essential amino acids needed for cell growth, and this deficiency may lead to cell death.[54]

Table 1: The qualitative phytochemical constituents of *T. catappa* methanol leaf extract

Phytochemical constituent	Test performed	Inference
Tannins	Ferric chloride test	+
Saponins	Froth test	+
Flavonoids	Ferric chloride test	+
Alkaloids	Mayer`s test	+
Phenolic compounds	Ferric chloride test	+
Anthraquinones	Borntrager`s test	+
Triterpenoids	Sulphuric acid test	+
Reducing sugar	Fehling`s test	+

+ = mean present

Table 2: UV-Vis spectrum peak values of the *T. catappa* methanol leaf extract

SN	Wavelength (nm)	Absorption Peak	Absorption Peak	Absorption Peak
		0.01mg/10 mL	0.02 mg /10 mL	0.03 mg /10 mL
1	200	1.198	0.790	1.091
2	250	0.794	1.002	0.752
3	300	1.377	1.532	1.400
4	350	1.590	1.315	1.424
5	400	1.004	0.850	0.983
6	650	1.389	2.558	1.741
7	750	1.836	2.367	2.146
8	800	1.305	1.874	1.759

This study also employed the UV-Vis approach to identify molecules containing lone pairs of electrons, pi-bonds, σ-bonds, chromophores, and aromatic rings in the UV-Vis area of the electromagnetic spectrum, thereby verifying the presence of phytochemicals or secondary metabolites. The *T. catappa* methanol extract's UV-Vis profile (Table 2), was chosen from 200 to 800 nm because of its broad range of distinguishing peaks and appropriate baseline.

The UV-Vis results revealed the presence of 8 peaks at 200, 250, 300, 350, 400, 650, 750, and 800 nm with absorption ranging from 0.752 to 2.558 a.u., as shown in Table 2. It has been stated that the peaks at 200, 250, 300, and 350 nm are flavonoids and their derivatives and that their occurrence ranges from 230 to 290 nm (band I) and 300 to 350 nm (band II).[55] According to Johnson and Syed[56], phenolic compounds and their derivatives are characterized by the presence of peaks between 280 and 330 nm. Thus, this implies that the *T. catappa* extract contains phenolic compounds and their derivatives. The peaks at 400 nm and 650 nm indicate that the extract contains terpenoids and chlorophyll since UV-Vis analysis with absorption bands at 400-550 nm and 600-700 nm shows the presence of terpenoids and chlorophyll.[55,56]

The methanol leaf extract of *T. catappa* was subjected to GC-MS analysis, which revealed the presence of 12 compounds, with 5 major prominent compounds (Table 3). Identification of bioactive chemicals, acids, volatile matter, branched chain hydrocarbons found in medicinal plants, alcohols, esters, and long-chain fatty acids can be achieved by combining gas chromatography and mass spectrometry. The GC-MS chromatogram of the *T. catappa* extract is displayed in Figure 1. Twelve compounds were found in all, five of which were major and seven minor (Table 3), and their structures are shown in Figure 2**.** The five prominent compounds constitute 70.49% of the extract of *T. catappa*. The 5 compounds and their % abundance are 9,17-Octadecadienal, (Z)- (23.18%), Epilupeol 20 [29]-Lupen-3alpha-ol, acetate (22.46%), 5-Hydroxy-1-(4-hydroxy-3-methoxyphenyl) decan-3-one (10.05%), n-Hexadecanoic acid (7.56%), and 1-(4-Hydroxy-3-methoxyphenyl)dec-4-en-3-one (7.24%). These prominent compounds were represented by peak numbers of 2, 6, 5, 1, and 4 with retention times of 8.237, 9.501, 9.415, 7.235, and 8.935, respectively.

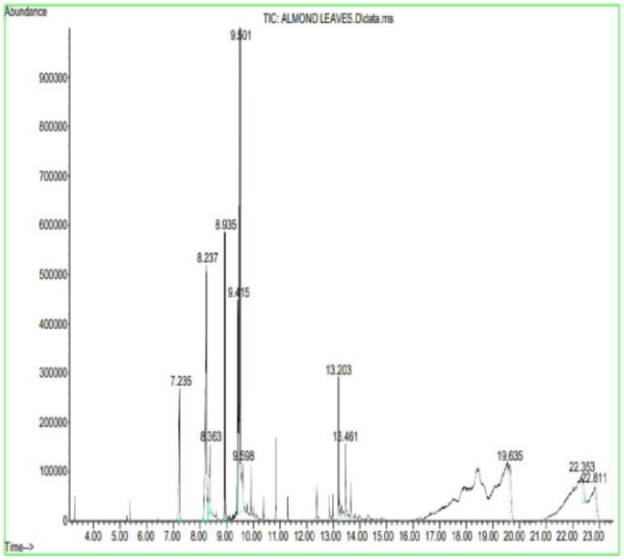

Figure 1: GC-MS Chromatogram of methanol extract of *T. catappa*

The high percentage of 9, 17-Octadecadienal ($C_{18}H_{32}O$) in the methanol extract of *T. catappa* may be responsible for the antibacterial activities of the plant because a study has shown that the compound has antimicrobial activity.[57] 5-Hydroxy-1-(4-hydroxy-3-methoxyphenyl) decan-3-one is also called gingerol and is one of the active components found in ginger. In one of our research projects, we observed that aqueous ginger extract showed poor antibacterial activity against *Staphylococcus aureus* and *Escherichia coli*.[58] The hexadecanoic acid found in the extract has been shown to have antifungal, antibacterial, and anti-inflammatory activities.[34] UV-Vis absorption techniques were used to examine the optical characteristics of *T. catappa* /ZnO-NPs.

ISSN 2616-0684 (Print)
ISSN 2616-0692 (Electronic)

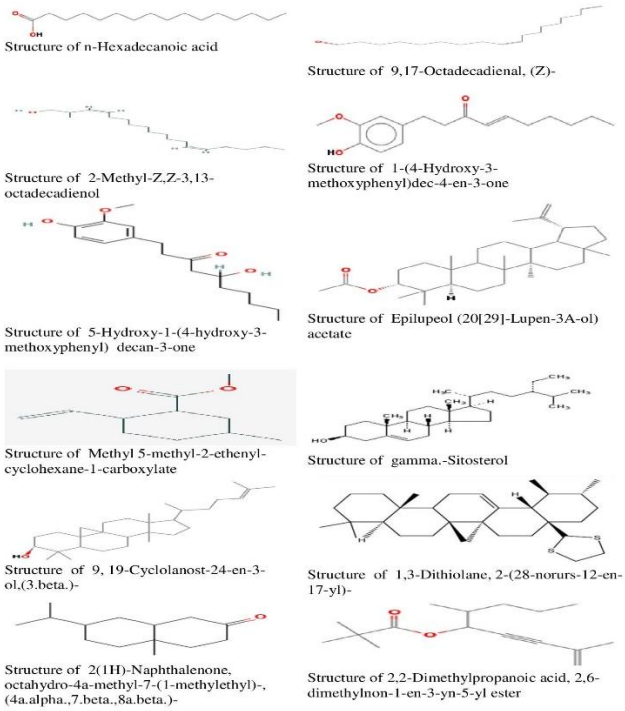

Figure 2: Structure of compounds obtained using GC-MS analysis of methanol extract of *T. catappa*

The production of *T. catappa*/ZnO-NPs from the methanol leaf extract of *T. catappa* was verified by the existence of the absorbance band between 250 and 430 nm.[7] Figure 3 illustrates the UV-Vis absorption spectra, which show a distinct absorption band at about 370 nm. This absorption band is caused by electron transitions from the valence band to the conduction band, which is linked to the fundamental band gap energy of ZnO crystals.

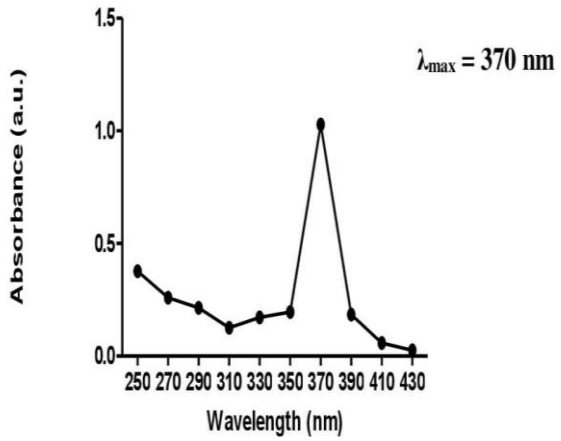

Figure 3: UV-Vis spectrum of ZnO-NPs prepared using *T. catappa* methanol extract.

In this study, the phytochemicals found in the methanol leaf extract of *T. catappa* were used as capping, reducing, and stabilizing agents for preparing *T. catappa*/ZnO-NPs. During the biosynthetic process, zinc ions were reduced to neutral zinc atoms, which led to the nucleation and development of ZnO-NPs. ZnO-NPs and non-oxidized ZnO-NPs with defects were biosynthesized as a result of the extract's bioactive constituents. Research has indicated that ZnO-NPs produced from extracts from *Artocarpus gomezianus, Euphorbia hirta, and Cassia fistula* were estimated to exhibit a redshift of approximately 5 nm.[59–61] Zinc oxide nanoparticles' optical band gap energy was determined using the following formula (Eqn.1):

$$\mathbf{E}=\frac{hc}{\lambda} \qquad \text{(Eqn 1)}$$

Where; h=6.626 × 10^{-34} Js, which is the Plancks constant, c is the velocity of light (3 × 10^{8} m/s), and λ is the wavelength with a value of 370 nm. The band gap energy of the synthesized zinc oxide nanoparticles was calculated to be 3.353 eV. The band at 370 nm indicates the production of hexagonal wurtzite zinc oxide and also shows the development of a considerable number of O-Zn^{2+} tetrahedrons.[62] When comparing the absorption peak (370 nm) to the bulk zinc oxide (365 nm), a redshift of -5 nm was seen.[63] The observed shift may be explained by shallow levels (the existence of oxygen defect states) inside the band gap and the large percentage of O_2 concentration (54.93%) in zinc oxide relative to zinc (36.14%).[64] Also, the morphological uniformity and chemical makeup of nanoparticles that have been biosynthesized were examined using SEM-EDX. Figure 4 displays the SEM micrographs and the findings of the EDX investigation of the *T catappa*/ZnO-NPs, which were produced under ideal conditions using *T. catappa* methanol extract. A good representative SEM image of the ZnO-NPs sample is shown in Figure 4(a–c).

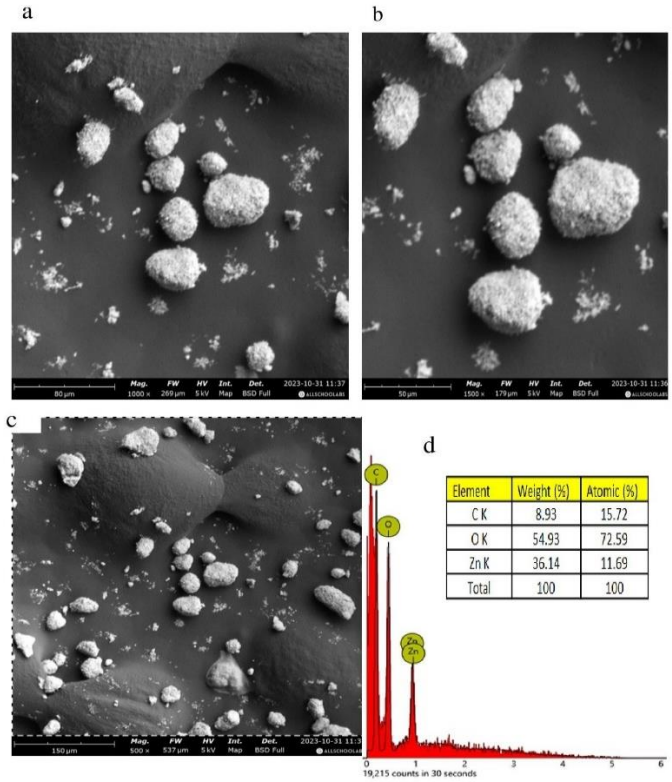

Figure 4: SEM images **(a-c)** and EDX spectrum and quantitative analysis of ZnO-NPs biosynthesized using *T. catappa* methanol extract **(d).**

These images show that the synthesized nanomaterial was dense and agglomerated (gathered into a ball, mass, or cluster), with irregular particle morphology and a quasi-spherical shape. Using EDX, ZnO-NP purity was also examined. The elemental composition of ZnO-NPs was ascertained by EDX analysis, as shown in Figure 4d. The spectrum produced by the EDX study showed the characteristic peaks for oxygen and zinc. The percentage weights of zinc and oxygen were determined to be 36.14% and 54.93%, respectively, based on the EDX spectra, which showed the presence of distinct peaks for both zinc and oxygen. These demonstrated the production of pure ZnO-NPs from *T. catappa's* methanol extract.

ISSN 2616-0684 (Print)
ISSN 2616-0692 (Electronic)

Table 3: Chemical composition of methanol leaf extract of *T. catappa*

PK no	RT	Name of compound	Molecular Formulae	Molecular Weight (g/mol)	Peak Area (%)	Ref#	CAS#	Qua
1	7.235	n-Hexadecanoic acid	$C_{16}H_{32}O_2$	256.4241	7.56	143510	000057-10-3	94
2	8.237	9,17-Octadecadienal, (Z)-	$C_{18}H_{32}O$	264.4461	23.18	153472	056554-35-9	95
3	8.363	2-Methyl-Z,Z-3,13-octadecadienol	$C_{19}H_{36}O$	280.50	4.41	173706	1000130-90-5	70
4	8.935	1-(4-Hydroxy-3-methoxyphenyl)dec-4-en-3-one	$C_{17}H_{24}O_3$	276. 3707	7.24	168685	000555-66-8	99
5	9.415	5-Hydroxy-1-(4-hydroxy-3-methoxyphenyl) decan-3-one	$C_{17}H_{26}O_4$	294.40	10.05	191534	039886-76-5	95
6	9.501	Epilupeol 20[29]-Lupen-3alpha-ol,acetate	$C_{32}H_{52}O_2$	468. 7541	22.46	331419	1010513-01-8	43
7	9.598	Methyl 5-methyl-2-ethenyl-cyclohexane-1-carboxylate	$C_{11}H_{18}O_2$	182.26	3.43	56685	1000144-54-1	53
8	13.203	gamma.-Sitosterol	$C_{29}H_{50}O_2$	414.7067	5.24	310598	000083-47-6	59
9	13.461	9,19-Cyclolanost-24-en-3-ol,(3.beta.)-	$C_{30}H_{50}O$	426.7174	3.25	316525	000469-38-5	94
10	19.635	1,3-Dithiolane, 2-(28-norurs-12-en-17-yl)-	$C_{32}H_{52}S_2$	500.89	6.12	338096	010153-89-6	38
11	22.353	2(1H)-Naphthalenone, octahydro-4a-methyl-7-(1-methylethyl)-, (4a.alpha.,7.beta.,8a.beta.)-	$C_{14}H_{24}O$	208.34	2.50	85288	054594-42-2	87
12	22.811	2,2-Dimethylpropanoic acid, 2,6-dimethylnon-1-en-3-yn-5-yl ester	$C_{16}H_{26}O_2$	250.3764	4.56	136003	1000299-33-6	32

Table 4: FTIR peak value related functional groups and phytocompounds in the *T. catappa* mediated ZnO-NPs

SN	Wave number cm^{-1} (reference article)	Wave number (cm^{-1}) for *T. catappa*	Functional group Assignment	Intensity	Phytocompound identified
1	3550-3200	3287.51197	O-H Stretching	83.81438	Alcohol
2		2344.49550	C-H stretching	92.77462	Aromatic aldehydes
3	-	2113.40055	-	93.98595	Unknown
4	2000-1650	1990.39841	C-H Bending	94.75427	Aromatic compound
5	2000-1650	1654.93800	C-H Bending	87.57402	Aromatic compound
	1610-1680		C=C stretch		Alkene
6	1550–1475 1475-1550	1546.84520	N-O asymmetric stretch	74.45133	Nitro compound
7	1440-1395	1435.02507	O-H bending	64.21308	Carboxylic acid
	1340-1470		C-H bend		Alkanes
8	1085-1050 1000-1150	1084.65531	C-O stretching C-F stretch	87.13735	Primary alcohol alkyl halides
9		868.46972	C-H Bending	83.17930	Aromatic compound
	650-1000		C-H bend		alkenes
10	730-665 650-1000	708.19419	C=C bending	84.71747	Alkenes

The structural properties, like crystallite size and strain, of the prepared *T. catappa*/ZnO-NPs synthesized from almond extract were investigated via XRD. The x-ray diffraction examination of the *T. catappa*/ZnO-NPs produces a plot of intensity versus the angle of diffraction. Figure 5(a) shows the x-ray diffraction pattern of the ZnO-NPs in the 2θ range of 30º-80º. The characteristic peaks at 31.70º, 34.40º, 36.22º, 47.46º, 56.58º, 62.54º, 66.32º, 67.42º, 69.40º, 72.14º, and 77.48º were attributed to the (100), (002), (101), (102), (110), (103), (200), (112), (201), (004), and (202) Bragg reflection planes, respectively. The obtained XRD pattern of our result was compared to the conventional zinc oxide pattern using JCPDS Reference Number 00-036-1451. The produced ZnO-NPs' wurtzite hexagonal crystal structure was revealed by the value. The highly crystalline nature of the nanoparticles was suggested by the sharp and narrow peaks. With the aid of the Debye-Scherrer formula, the nanoparticles' crystallite size was determined.

$$D = K\lambda/\beta \mathrm{Cos}\theta \qquad \text{(Eqn. 2)}$$

ISSN 2616-0684 (Print)
ISSN 2616-0692 (Electronic)

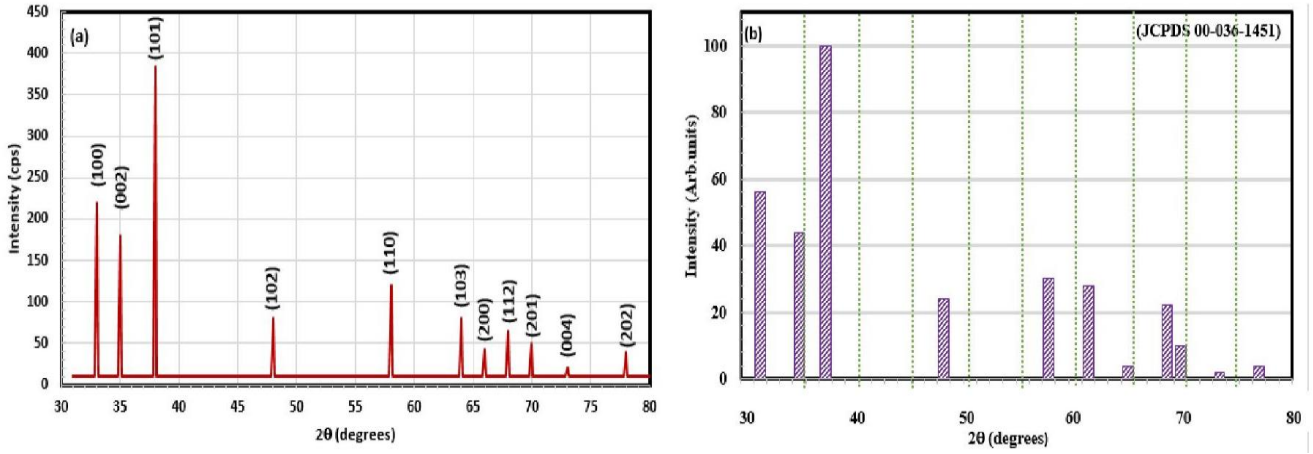

Figure 5: XRD plots of *T. catappa* /ZnO-NPs: (a) full-degree scale and (b) standard ZnO-NPs particles

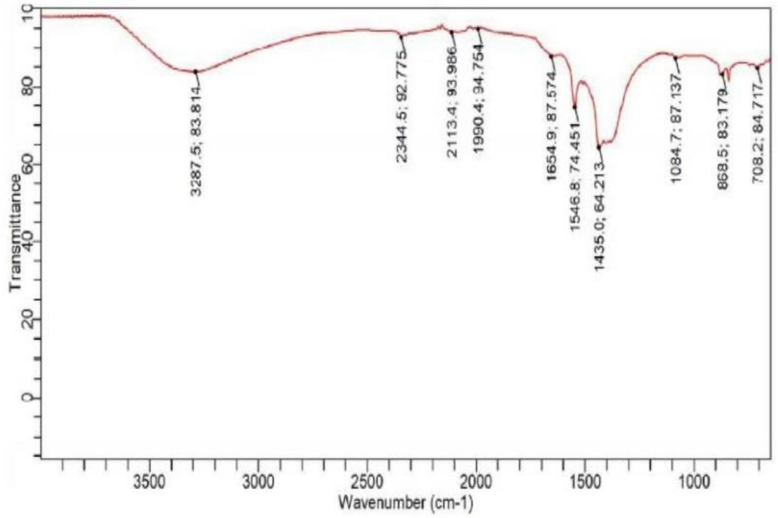

Figure 6: FTIR spectrum of ZnO-NPs produced from *T. catappa* methanol extract

The above equation, where D is the zinc oxide nanoparticles' crystalline size, K is the Scherrer constant (0.89), λ is the wavelength (1.54056 Å), θ is the Bragg angle in radians, and β is the ZnO-NPs' full width at half maximum (FWHM), was used to determine the nanoparticles' crystalline size. The crystalline hexagonal Wurtzite particle structure was confirmed by the XRD spectrum. Equation 2 was used to determine the average crystallite size D, which came out to be 53.46 nm. The conventional hexagonal Wurtzite crystal structure of ZnO-NPs is confirmed by the diffraction pattern of ZnO-NPs synthesized from *T. catappa*; these results are in agreement with those previously reported in other investigations.[7,8] The number of dislocation lines per unit volume of the crystal, or the size of the crystal defects the crystal possesses, is indicated by the dislocation density value (δ_{np}). Stated otherwise, the ZnO nanoparticle profile's degree of crystallinity will be shown by the dislocation density value. The dislocation density (δ_{np}) of the ZnO-NPs that were produced was determined by applying the formula.

$$(\delta_{np}) = 1/D^2 \qquad \text{(Eqn 3)}$$

D is the crystallite size. For the ZnO-NPs produced in this research, the dislocation density averaged 0.000349899 $(nm)^{-2}$ was obtained. The dislocation density (δ_{np}) of the nanoparticle is small, and the small dislocation density value indicates that the ZnO-NPs produced have a high degree of crystallinity.

FTIR was used to analyze the functional group of the ZnO-NPs surface mediated by *T. catappa*. Research has indicated that phytochemicals found in plant extracts can stabilize ZnO-NPs by decreasing Zn^{2+} ions.[65] Ten distinct peaks were revealed by FTIR analysis of ZnO nanoparticles made from *T. catappa* leaf extract (Table 4). Figure 6 indicates a wide band of O-H stretching of intermolecular bonds with peaks at 3287.512 cm^{-1} (3550-3200 cm^{-1}).[8] The absorption peak at 2344.49550 cm^{-1} was ascribed to the C-H stretching of aromatic alkanals.[8] The band that falls within the range of 2000-1800 cm^{-1} (1990.40) was due to the weak C-H bending of aromatic compounds.[7] Rani *et al*. (2021),[66] study shows that 1654.94, 1546.85, 1435.025, and 708.19 cm^{-1} have C-H bending, nitrogen-oxygen asymmetric stretch, oxygen-hydrogen bending, and C=C bending with aromatic, nitro, carboxylic acid, and alkene functional groups, respectively.[66] A band at 1084.66 cm^{-1} may be due to the carbon-oxygen and carbon-carbon extended vibrations and carbon-hydrogen twist of starch.[67] A study has shown that distinct bands at 1029.61 cm^{-1} and 1084.85 cm^{-1} could be due to the presence of carbon-oxygen stretching vibration due to secondary alkanol or an ester group.[56] The band at 868.47, close to 881 cm^{-1} obtained by Rad *et al*.[68] was shown to be an aromatic organic ring and the functional group present in some organic compounds. Theng and Korpenwar's,[47] study shows that identified bands at 1654.94 (1610-1680), 1546.85 (1475-1550), 1435.025 (1340-1470), 1084.66 (1000-1150), 868.47 (650-1000), and 708.19 (650-1000) cm^{-1} could be due to the presence of carbon-carbon double bond stretch, nitrogen-oxygen asymmetric stretch, carbon-hydrogen bend, C-F stretch, C-H bending, and C=C bending leading to an alkene, nitro compound, alkanes, alkyl halides, alkenes, and alkenes functional groups, respectively. FTIR examination of the ZnO-NPs generated from *T. catappa's* methanol leaf extract revealed the presence of functional groups such as alkanol, aromatic aldehydes, aromatic compounds, nitro compounds, alkanoic acids, alkyl halides, alkanes, and alkenes.

ISSN 2616-0684 (Print)
ISSN 2616-0692 (Electronic)

The occurrence of all these compounds on the surface of the ZnO-NPs revealed that the nanoparticles contain a plethora of phytochemicals. The proposed mechanism of the synthesized *T. catappa* /ZnO nanoparticles is shown in the equations below;

(a) $Zn(CH_3COO)_2.6H_2O + 2NaOH \rightarrow Zn(OH)_2 + 2CH_3COONa + 6H_2O$ Eqn. 4

(b) $Zn(OH)_2 + 2CH_3COONa + 6H_2O \xrightarrow{\text{Plant extract}} \text{ZnO-Nanoparticles}$ Eqn. 5

During the creation of zinc oxide nanoparticles, phenolic compound derivatives like flavonoids and thymol found in plant extracts function as size-reducing agents to inhibit further growth of zinc oxide crystals. Carboxylic and hydroxyl groups that are present in phenol derivatives found in plant extract are linked to the surface of ZnO nanoparticles, where they act as stabilizers, surfactants, capping agents, and size reducers.[69]

DPPH and FRAP radical scavenging activities of T. catappa extract and biosynthesized ZnO-NPs

Antioxidants are substances that scavenge reactive oxygen species (ROS) by inhibiting oxidative reactions, thereby shielding cells from the detrimental effects of ROS overproduction. Numerous naturally occurring substances found in plants and their extracts have the potential to function as antioxidants because of their effective capacity to mitigate ROS-mediated pathogenesis of several degenerative diseases, including cancer and cardiovascular ailments. Several metabolic activities require large quantities of natural antioxidant molecules. Natural antioxidant molecules are in high demand for different metabolic processes.[70,71] DPPH, total antioxidant capacity (TAC), and total reducing power (TRP) are some of the different tests used to verify the antioxidant capacity of biosynthesised ZnO-NPs. The potential of antioxidants found in varieties of foods, such as vegetables, juices, plant extracts, and biosynthesized nanoparticles, is tested using these techniques. These methods are very sensitive, easy to use, and not expensive.[72]

As the concentration of the *T. catappa* extract and ZnO-NPs increased, the absorbance of the DPPH decreased at 517 nm. The mechanism of reaction showed that the DPPH free radical contains an odd electron based on the n→π* transition, and the *T. catappa* extract and the synthesized ZnO-NPs transfer electrons from the oxygen atom to the nitrogen atom of DPPH, leading to suppression of oxidation (Figure 7). The *in vitro* antioxidant activity evaluated by antioxidant assay demonstrated that the extract and ZnO-NPs showed prominent antioxidant properties. The concentrations of the *T. catappa* extract and ZnO-NPs showed 50 percent inhibition (IC_{50}) of DPPH scavenging activity at 79.50 µg/mL and 59.86 mg/mL, respectively (Figures 8a and 8b). The *T. catappa* extract showed better DPPH radical scavenging properties when compared to the ZnO-NPs. Bikanga *et al*.[43] research work shows that ethanol extract of *T. catappa* has DPPH scavenging activity with IC_{50} = 0.270±0.144 mg/mL.

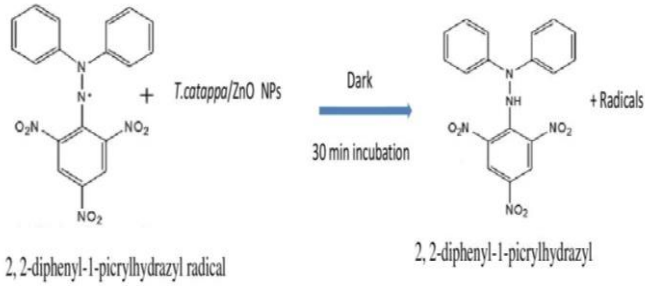

Figure 7: The mechanism of action for DPPH radical scavenging activity of *T. catappa* extract and ZnO-NPs

The capacity of antioxidant substances to reduce the oxidative damage of reactive oxygen species (ROS) is measured by the FRAP test. Antioxidants' capacity to reduce Fe^{3+}, or ferricyanide complex, to the iron (ii) cation, or ferrous form (Fe^{2+}), is the basis for this test. By monitoring Perl's Prussian blue production at 700 nm, the reduction process can be ascertained. Increased ferric-reducing power is typically indicated by increased absorbance. A rise in absorbance signifies a rise in reductive capacity. As seen in Figure 9, the FRAP increases in this order: ZnO-NPs< *T. catappa* extract< ascorbic acid.

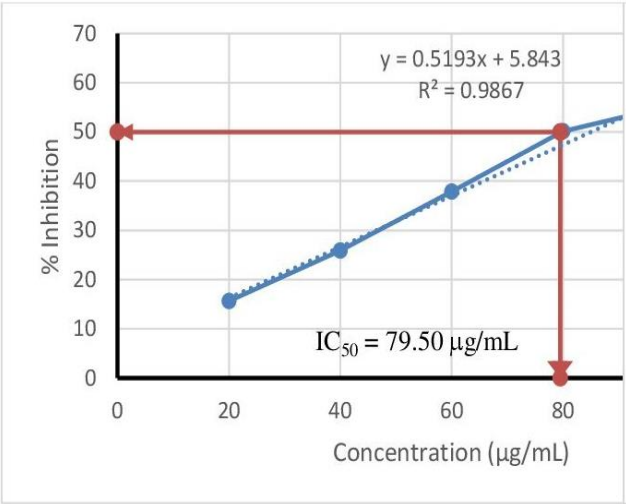

Figure 8a: DPPH radical scavenging activity of *T. catappa* methanol leaf extract

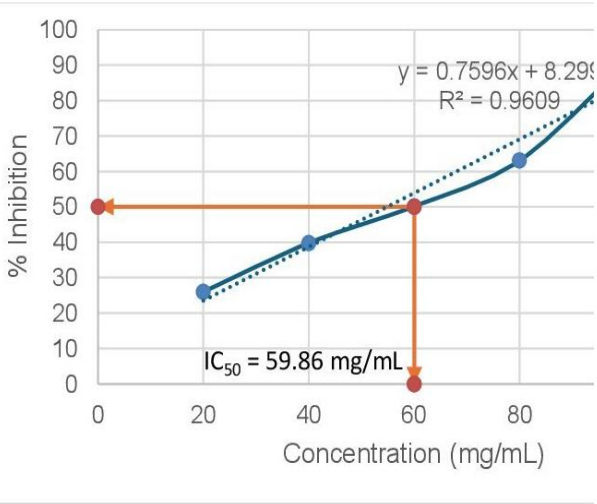

Figure 8b: DPPH radical scavenging activity of ZnO-NPs

ISSN 2616-0684 (Print)
ISSN 2616-0692 (Electronic)

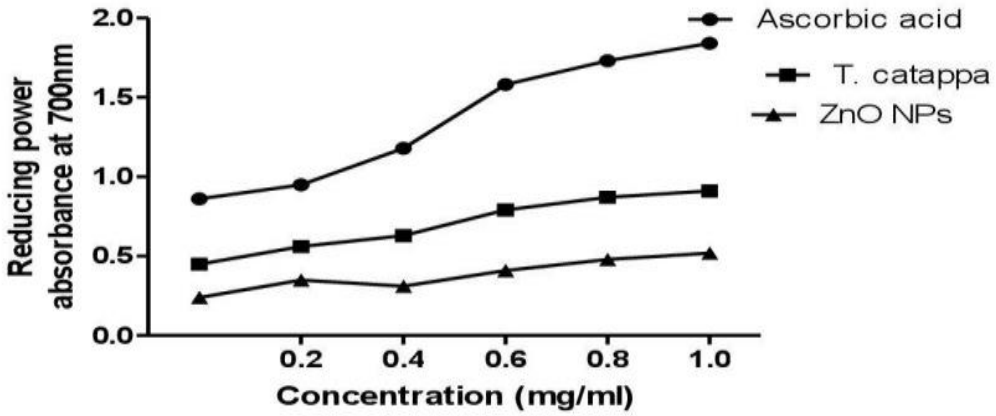

Figure 9: Reducing power of ascorbic acid, *T. catappa* extract, and ZnO-NPs at different concentrations. Each value represents mean ± SD (n = 3)

Plant-based antibacterial agents play a crucial role in supplying novel compounds to chemists, enabling them to enhance bioactivity through research into the chemical and pharmacological activities of antibacterial plants and their potential utility in the development of novel drugs that combat antibiotic-resistant bacteria. In this study, the antibacterial activity of *T. catappa* methanol extract and ZnO-NPs produced from *T. catappa* methanol extract against four Gram-negative bacteria strains (*E. coli*, *S. typhi*, *K. pneumonia*, and *P. aeruginosa*) and one Gram-positive bacteria strain (*S. aureus*) was studied using the agar well diffusion method (Figure 10 a-h).

The extract of *T. catappa* showed a strong antibacterial response against *S. aureus*, *P. aeruginosa*, and *E. coli* with zones of inhibition of 21.33±0.38, 23.54±0.78, and 23.66±0.43 mm at 100 mg/mL and 24.00±0.85, 27.33±0.93 and 28.50±1.23 mm at 200 mg/mL, respectively. These microorganisms are highly susceptible to the extract. At 100 and 200 mg/mL *K. pneumoniae* and *S. typhi* showed moderate and strong responses with zones of inhibition of 20.43±0.42, 18.36±0.65, 25.75±0.86, and 21.66±1.46 mm, respectively (Table 5).

Table 5: Zone of inhibition for *T. catappa* methanol extract, ZnO-NPs, and tetracycline solution against Gram-negative and Gram-positive bacteria

Test organisms	Zone of inhibition for methanol leaf extract of *T. catappa* at 100 mg/mL (mm)	Zone of inhibition for methanol leaf extract of *T. catappa* at 200 mg/mL (mm)	Zone of inhibition for ZnO-NPs at 1 mg/mL (mm)	Zone of inhibition for tetracycline solution at 30 mg/mL (mm)
Escherichia coli	23.66±0.43^{a}	28.50±1.23^{a}	16.33±0.36^{a}	33.33±0.84^{b}
Staphylococcus aureus	21.33±0.38^{b}	24.00±0.85^{bc}	11.63±0.43^{c}	29.03±0.70^{d}
Salmonella typhi	18.36±0.65^{d}	21.66±1.46^{c}	13.58±0.72^{b}	32.40±0.66^{c}
Klebsiella pneumonia	20.43±0.42^{c}	25.75±0.86^{ab}	15.70±0.53^{a}	34.68±0.56^{ab}
Pseudomonas aeruginosa	23.54±0.78^{a}	27.33±0.93^{a}	13.83±0.96^{b}	35.30±0.82^{a}

Data represent means ± SD. a=highest, c= medium, d=lowest. Those alphabets that have different letters across each column are statistically significant (p<0.05).

The Gram-negative bacteria (*E. coli* and *P. aeruginosa*, with a p-value of 0.001) were more susceptible to *T. catappa* extract at both concentrations when compared to the Gram-positive bacterium, as shown in this study. In research carried out by Muthulakshmi and Neelanarayanan,[44] the antibacterial activities of ethanol, methanol, petroleum ether, and aqueous extracts of *T. catappa* were evaluated against five different bacterial pathogens such as *P. aeruginosa*, *P. mirabilis*, *K. pneumoniae*, *S. aureus*, and *S. paratyphi A* at four different concentrations (standard drug, 100 µL, 250 µL, and 500 µL) of the test samples, of all the antimicrobial tests carried out, the highest antibacterial activity was observed with methanol, ethanol, aqueous, and petroleum ether extracts of *T. catappa* against *K. pneumonia* (29±0.57, 28.67±0.66, 27±1.00, 25.67±0.33) in 500 µL concentrations, respectively. In another study, it was observed that the isolated fraction from *T. catappa* showed antimicrobial activity, with the most sensitive being Methicillin-resistant *Staphylococcus aureus*, and *Staphylococcus aureus* at 0.097 mg/mL, while the fungi *Candida albicans* and *Trichophyton rubrum* were inhibited at 0.097 mg/mL, respectively.[45]

The zinc oxide nanoparticles used in the experiment at 1 mg/mL concentration against *S. aureus*, *S. typhi*, *P. aeruginosa*, *K. pneumonia*, and *E. coli* exhibited weak and moderate antibacterial activities with zones of inhibition of 11.63±0.43, 13.58±0.72, 13.83±0.96, 15.70±0.53, and 16.33±0.36 mm, respectively. *E. coli* and *K. pneumonia* (p-value of 0.001) were more susceptible to the ZnO-NPS synthesized from *T. catappa* extract when compared to *S. aureus*. It is expected that the bio-functionalized ZnO-NPs should be more active against *E. coli* compared to *S. Aureus* since Gram-negative bacteria contain a thin peptidoglycan layer, a heteropolysaccharide that contains monomers of repeating N-acetylglucosamine and N-acetylmuramic acid residues joined by *β*-1-4-glycosidic bonds. Awe *et al.*[73] study shows that ZnO-NPs synthesized from *T. catappa* exhibited antibacterial activities against *S. aureus*, *E. coli*, *P. aeruginosa*, and *S. typhi*, with zones of inhibition of 29, 25, 30, and 26 mm, respectively. ZnO nanoparticles'

ISSN 2616-0684 (Print)
ISSN 2616-0692 (Electronic)

Figure 10a: Zone of inhibition at 200 mg/mL for methanol extract of *T. catappa* against *K. pneumonia.*

Figure 10b: Zone of inhibition at 200 mg/mL for methanol extract of *T. catappa* against *P. aeruginosa.*

Figure 10c: Zone of inhibition at 200 mg/mL for methanol extract of *T. catappa* against *E. coli*

Figure 10d: Zone of inhibition at 200 mg/mL for methanol extract of *T. catappa* against *S. aureus.*

Figure 10e: Zone of inhibition at 200 mg/mL for methanol extract of *T. Catappa* against *S. typhi.*

Figure 10f: Zone of inhibition at 30 mg/mL for tetracycline against *S. aureus.*

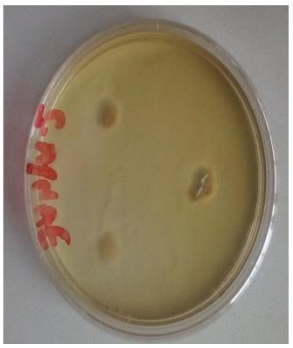

Figure 10g: Zone of inhibition at 1 mg/mL for ZnO-NPs against *S. typhi*

Figure 10h: Zone of inhibition at 1 mg/mL for ZnO-NPs against *E. coli*

exceptional antibacterial activity may be attributed to many reasons, each of which might be examined separately. Firstly, research has shown that ZnO nanoparticles have high surface energy, which enhances their ability to adhere to bacterial cell walls.[74] Secondly, the ZnO nanoparticle has an electrical effect and can easily penetrate the bacterial cell wall with ease.[75] The third and most significant reason for the antibacterial activity of ZnO-NPs is the formation of ROS. ROS, also known as secondary active agents, change the membrane's penetrability, causing proteins and lipids to be released from the cell and ultimately causing microbial cells to die.[76] Lastly, the nanostructured zinc oxide nanoparticles allow the production of reactive oxidative free radicals that damage the bacterial cell wall.[77] The larger K^+ ion gradient inside the bacterial cell, which holds the cellular matrix in place, is lost when the cell walls are damaged. A K^+ ion deficit stops respiration, cell division, and other metabolic functions. This eventually causes the death of the bacterial cell.[77] The extract showed stronger antibacterial activity against the tested bacteria compared to the synthesized ZnO-NPs. The tetracycline solution used at 30 mg/mL against *S. aureus, S. typhi, E. coli, K. pneumonia,* and *P. aeruginosa* exhibits strong and potent antibacterial activities with zones of inhibition of 29.03±0.70, 32.40±0.66, 33.33±0.84, 34.68±0.56 and 35.30±0.82 mm, respectively. *K. pneumonia and P. aeruginosa* (p-value of 0.001) were more susceptible to tetracycline (Table 5). MIC is the lowest concentration of an antimicrobial agent needed to stop a microorganism from growing visible. Based on the degree of turbidity in the *T. catappa* methanol extract dilution, the MIC value was calculated. The MIC of *T. catappa* methanol extract was assessed in this investigation against five different bacteria. The result in Table 6 showed that the *T. catappa* extract showed antibacterial activity against *S. aureus, S. typhi, P. aeruginosa, K. pneumonia,* and *E. coli* with MIC and MBC values of 25, 25, 12.50, 12.50, 12.50, and 50, 50, 25, 25, and 25 mg/mL, respectively. The MBC/MIC ratio obtained in our study for all the organisms tested was 2, and this is an indication that the *T. catappa* leaf extract has bactericidal effects on all the tested bacteria used in this study since their MBC/MIC values are less than 4. In a study carried out by Sowmya and Raveesha,[45] they observed that fraction TCAF2 from *T. catappa* exhibited very good inhibitory activity against all of the tested microorganisms, with MIC values ranging from 0.097 to 0.390 mg/mL. The most sensitive were MRSA 1503, *S. aureus* (clinical isolate), and *S. typhi* (MTCC 733), which had the lowest inhibitory concentration of 0.097 mg/mL. With MICs of 0.390, 0.195, and 0.781 mg/mL, respectively, MRSA 1007, *S. aureus* (MTCC 7443), and *P. vulgaris* (clinical isolate) had moderate inhibitory action.[45] The MBC values for the bacteria tested range from 6.25 to 25 mg/mL. *P. vulgaris* (clinical isolates) and *S. aureus* exhibited MBCs at 25 and 0.39 mg/mL, respectively. MRSA 1007 and MRSA 1503 exhibited bactericidal effects at 6.25 and 25 mg/mL, while *S. typhi* (MTCC 733) and *S. aureus* (MTCC 7443) exhibited bactericidal properties at 0.78 and 12.25 mg/mL, respectively.[45]

Table 6: MIC and MBC for *T. catappa* extracts against Gram-negative and Gram-positive bacteria

Test organisms	*Staphylococcus aureus*	*Escherichia coli*	*Klebsiella pneumoniae*	*Salmonella typhi*	*Pseudomonas aeruginosa*
MIC for methanol extract of *T. catappa* (mg/mL)	25	12.50	12.50	25	12.50
MBC for methanol extract of *T. catappa* (mg/mL)	50	25	25	50	25
MBC/MIC for *T. catappa*	2	2	2	2	2

Conclusion

This study demonstrates the production of ZnO-NPs using an eco-friendly *T. catappa* methanol extract. The extract serves as a reducing and capping agent for the production of ZnO-NPs. The phytochemical screenings of the plant showed that it contains important phytochemicals serving as strong capping and stabilizing agents. The GC-MS analysis of the leaf extract of *T. catappa* revealed the presence of 12 different compounds, with 9, 17-Octadecadienal (Z) compound as the major component. The UV-vis spectrum demonstrated a distinct band for the synthesized hexagonal pure ZnO. The SEM shows irregular ZnO-NPs morphology, a quasi-spherical-like shape that is dense and agglomerated; while the EDX indicates that the ZnO-NPs contain zinc and oxygen as the major elements. The FTIR analysis shows that the synthesized ZnO-NPs contain some important phytochemicals responsible for their biological properties. The *T. catappa* extract and the biosynthesized ZnO-NPs exhibited notable antioxidant activity; they also showed antibacterial properties against specific microorganisms. The aforementioned findings demonstrated that biosynthesized ZnO-NPs can significantly advance a wide range of biological applications.

Conflict of interest

The authors declare no conflict of interest.

Authors' Declaration

The authors hereby declare that the work presented in this article are original and that any liability for claims relating to the content of this article will be borne by them.

Acknowledgements

The authors are grateful to Alimat Iseoluwapo Odetayo, Olaoluwa Esther Tunrayo, Aishat Ayomide Ajibade, and Mariam Gbemisola Osungbemi for their assistance when carrying out the laboratory work.

References

1. Mahendra C, Murali M, Manasa G, Ponnamma P, Abhilash MR, Lakshmeesha TR, Satish A, Amruthesh KN, Sudarshana MS. Antibacterial and antimitotic potential of bio-fabricated zinc oxide nanoparticles of *Cochlospermum religiosum (L.)*. Microb. Pathog. 2017;110: 620–629.
2. Singh AK, Pal P, Gupta V, Yadav TP, Gupta V, Singh SP. Green synthesis, characterization and antimicrobial activity of zinc oxide quantum dots using *Eclipta alba*. Mater. Chem. Phys. 2018;203: 40–48.
3. Luque-Morales PA, López-Peraza A, Nava-Olivas OJ, Amaya-Parra G, Báez-López YA, Orozco-Carmona VM, Garrafa-Gálvez HE, Chinchillas-Chinchillas MDJ. ZnO Semiconductor Nanoparticles and Their Application in Photocatalytic Degradation of Various Organic Dyes. Materials. 2021; 14:7537. doi.org/10.3390/ma14247537
4. Al-Zahrani SA, Patil MB, Mathad SN, Patil AY, Otaibi AA, Masood N, Mansour D, Khan A, Manikandan A, Syafri E. Photocatalytic Degradation of Textile Orange 16 Reactive Dye by ZnO Nanoparticles Synthesized via Green Route Using *Punica Granatum* Leaf Extract. Crystals. 2023; 13: 172. doi.org/10.3390/ cryst13020172
5. Xu L, Xian F, Zhang Y, Wang W, Qiu K, Xu J. Synthesis of ZnO-decorated SnO_2 nanopowder with enhanced photocatalytic performance. Optik. 2019; 194:162965. doi.org/10.1016/j.ijleo.2019.162965
6. Ali TT, Narasimharao K, Parkin IP, Carmalt CJ, Sathasivam S, Basahel SN, Bawaked SM, Al-Thabaiti SA. Effect of pretreatment temperature on the photocatalytic activity of microwave irradiated porous nanocrystalline ZnO. New J. Chem. 2015;39: 321–332.
7. Gaur J, Vikrant K**,** Kim KH, Kumar S, Pal M, Badru R, Masand S, Momoh J. Photocatalytic degradation of Congo red dye using zinc oxide nanoparticles prepared using *Carica papaya* leaf extract. Mater. Today Sustain**.** 2023;22: 100339 doi.org/10.1016/j.mtsust.2023.100339
8. Gaur J, Kumar S, Pal M, Kaur H, Supreet, Badru R, Momoh J, Pal R, Kumar S. Bio-engineered, phyto-decorated, multi-form *P. betel*/ZnO as a potential photocatalytic agent, Adv. Nat. Sci. Nanosci. Nanotechnol. 2023;14: 035014 doi.org/10.1088/2043-6262/acf28a
9. Gaur J, Kumar S, Pal M, Kaur H, Batoo KM, Momoh JO, Supreet. Current trends: Zinc oxide nanoparticles preparation via chemical and green methods for the photocatalytic degradation of various organic dyes. Hybrid Adv. 2024; 5: 100128. doi.org/10.1016/j.hybadv.2023.100128
10. Gaur J, Kumar S, Kaur H, Pal M, Supreet4, Bala K, Batoo KM, Momoh JO, Hussain S. Eco-friendly innovation: harnessing nature's blueprint for enhanced photocatalysis and antimicrobial potential in multi-structured PN/ZnO nanoparticles. Funct. Compos. Struct. 2024; 6: 015005 doi.org/10.1088/2631-6331/ad2c10
11. Thaya R, Malaikozhundan B, Vijayakumar S, Sivakamavalli J, Jeyasekar R, Shanthi S, Vaseeharan B, Palaniappan R. Chitosan coated Ag/ZnO nanocomposite and their antibiofilm, antifungal and cytotoxic effects on murine macrophages. Microb. Pathog. 2016;100: 124–132.
12. Rajakumar G, Thiruvengadam M, Mydhili G, Gomathi T, Chung III-M. Green approach for the synthesis of zinc oxide nanoparticles from *Andrographis paniculata* leaf extract and evaluation of their antioxidant, anti-diabetic, and anti-inflammatory activities. Bioprocess Biosyst Eng. 2018; 41:21–30. doi.org/10.1007/s00449-017-1840-9
13. Park C, Lee J, So HM, Chang WS. An ultrafast response grating structural ZnO photodetector with back-to-back Schottky

barriers produced by hydrothermal growth. J. Mater. Chem. C. 2015;3: 2737–2743.
14. Ohashi H, Hagiwara M, Fujihara S. Solvent-assisted microstructural evolution and enhanced performance of porous ZnO films for plastic dye-sensitized solar cells. J. Power Sources. 2017;342:148–156.
15. Vijayakumar S, Vaseeharan B, Malaikozhundan B, Shobiya M. *Laurus nobilis* leaf extract mediated green synthesis of ZnO nanoparticles: characterization and biomedical applications. Biomed. Pharmacother. 2016; 84:1213–1222.
16. Umar H. Morphological Changes Caused by Synthesized Zinc Oxide Nanoparticles in MDA-MB 231 Cells and Prediction with Multi-Linear Regression. Trop J Nat Prod Res. 2023; 7(12): 5616-5622. http://www.doi.org/10.26538/tjnpr/v7i12.36.
17. Vakulov ZE, Zamburg EG, Khakhulin DA, Ageev OA. Thermal stability of ZnO thin films fabricated by pulsed laser deposition, Mater. Sci. Semicond. Process. 2017;66:21–25.
18. Gaur J, Kumar S, Zineddine M, Kaur H, Pal M, Bala K, Kumar V, Lotey GS, Musa M, Outassi OE. CTAB-crafted ZnO nanostructures for environmental remediation and pathogen control. Sci Rep. 2024; 14: doi.org/10.1038/s41598-024-65783-x
19. Rashad MM, Ismail AA, Osama I, Ibrahim IA, Kandil AHT. Photocatalytic decomposition of dyes using ZnO doped SnO2 nanoparticles prepared by solvothermal method. Arab, J. Chem. 2014; 7 (1): 71–77.
20. Khan MF, Ansari AH, Hameedullah M, Ahmad E, Husain FM, Zia Q, Baig U, Zaheer MR, Alam MM, Khan AM, AlOthman ZA, Ahmad I, Ashraf GM, Aliev G. Sol-gel synthesis of thorn-like ZnO nanoparticles endorsing mechanical stirring effect and their antimicrobial activities: Potential role as nano-antibiotics. Sci Rep. 2016;6: doi: 10.1038/srep27689
21. Gan PP, Huang NY, Li SF. Green synthesis of gold nanoparticles using palm oil mill effluent (POME): a low-cost and eco-friendly viable approach. Bioresour. Technol. 2012;113: 132–135.
22. Benelli G, Lukehart CM. Special issue: applications of green-synthesized nanoparticles in pharmacology, parasitology, and entomology. J. Clust. Sci. 2017;28: 1–2.
23. Banumathi B, Vaseeharan B, Chinnasamy T, Vijayakumar S, Govindarajan M, Alharbi NS, Kadaikunnan S, Khaled JM, Benelli G. *Euphorbia rothiana*-fabricated Ag- nanoparticles showed high toxicity on *Aedes aegypti* larvae and growth inhibition on microbial pathogens: a focus on morphological changes in mosquitoes and antibiofilm potential against bacteria. J. Clust. Sci. 2017;28: 2857–2872.
24. Banumathi B, Vaseeharan B, Rajasekar P, Prabhu NM, Ramasamy P, Murugan K, Canale A, Benelli G. Exploitation of chemical, herbal and nano formulated acaricides to control the cattle tick, *Rhipicephalus (Boophilus) microplus* – a review. Vet. Parasitol. 2017;244: 102–110.
25. Halilu EM, Ngweh VA, Airemwen CO. Green Synthesis of Silver Nanoparticles from *Parinari curatellifolia* Methanol Stem Bark Extract and Evaluation of Antioxidant and Antimicrobial Activities. Trop J Nat Prod Res. 2023; 7(3):2498-2505. http://www.doi.org/10.26538/tjnpr/v7i3.5.
26. Fagbemi KO, Thonda OA, Daramola OO, Oyewole TE, Adeduro OO, Amodu S, Popola D, Aina DA. Antibacterial Activity of Silver Nanoparticles Synthesized Using *Vitex grandifolia* Against Multidrug-Resistant (MDR) Pathogens. Trop J Nat Prod Res. 2024; 8(8):8068-8074. https://doi.org/10.26538/tjnpr/v8i8.21.
27. Gholami-Shabani M, Shams-Ghahfarokhi M, Gholami-Shabani Z, Akbarzadeh A, Riazi G, Ajdari S, Amani A, Razzaghi-Abyaneh M. Enzymatic synthesis of gold nanoparticles using sulfite reductase purified from *Escherichia coli*: a green eco-friendly approach. Process Biochem. 2015;50: 1076–1085.
28. Saravanana M, Gopinathc V, Chaurasiab MK, Syedd A, Ameend F, Purushothamane N. Green synthesis of anisotropic zinc oxide nanoparticles with antibacterial and cytofriendly properties. Microb. Pathog. 2018;115: 57–63.
29. Imadea EE, Ajiboye TO, Fadiji AE, Onwudiwe DC**,** Babalola OO. Green synthesis of zinc oxide nanoparticles using plantain peel extracts and the evaluation of their antibacterial activity. Sci. Afr. 2022;16: doi: 10.1016/j.sciaf.2022.e01152
30. Abdurasid AA, Momoh JO, Aderele OR. Experimental and Mathematical Model for the Study of the *In-vitro* Susceptibility of Antimicrobial Agents against *Escherichia coli* Isolates Obtained from Abattoir Centres in Ikorodu, Lagos, Nigeria. Curr. J. Appl. Sci. Technol. 2018; 28(2):1-15.
31. Aderele OR, Kareem RA, Momoh JO**.** Phytochemical Screening, Mathematical Analysis and Antimicrobial Activity of Methanolic Seed Extract of *Hunteria Umbellata*. Euro. J. Med. Plants. 2020; 31(16): 1-17.
32. Momoh JO, Manuwa AA, Bankole YO. Phytochemical Screening, Atomic Absorption Spectroscopy, GC-MS, and Antibacterial Activities of Turmeric (*Curcuma longa* L.) Rhizome Extracts. J. Adv. Microbiol. 2022; 22(9): 116-131.
33. Momoh JO, Manuwa AA, Ayinde FA, Bankole YO. Nutritional, Phytochemicals, GC-MS and Antibacterial Activities of Aqueous Red Onion (*Allium cepa*) Extract against *Staphylococcus aureus* and *Escherichia coli.* Int.J.Trop. Dis. Healh. 2023; 44 (5): 35-51.
34. Momoh JO, Damazio OA, Oyegbami OM. GC–MS Analysis and Antimalarial Activity of Methanolic Leaf Extract of *Carica papaya* against *Plasmodium berghei NK65* Infection in Swiss Mice. Annu.Res. Rev.Biol. 2020; 35(12):183-197.
35. Momoh JO, Damazio OA, Ajetunmobi OA, Babalola AO, Adekunle MO, Busari NO, Musa AA. Phytochemical Analysis and Antiplasmodial (curative) Activities of Methanolic Leaf Extract of *Morinda lucida* (Ewe Oruwo) in Male Swiss Mice Infected with *Plasmodium berghei NK65*. Int.J.Trop. Dis. Healh. 2019; 37(1):1-13.
36. Salim HM, KurniaL F, Bintarti TW, Handayani H, Shimabukuro M. Hepatoprotective Effects of Methanol Extract of *Syzygium polyanthum* L. Leaves (Salam) on High Fat Diet. Trop J Nat Prod Res.2021; 5(12):2092-2095. doi.org/10.26538/tjnpr/v5i12.8.
37. Momoh JO, Adeniyi MO, Aderele OR. Experimental and Mathematical Model for the Hepatoprotective Effect of Methanolic Extract of *Moringa oleifera* Leaf against CCl_4-induced Hepatotoxicity in Sprague Dawley Male Albino Rats. J.Adv.Med. Med. Res. 2018; 26(5):1-14.
38. Momoh JO**,** Aderele OR, Kareem RA. Sub-acute and protective effect of *Cymbopogon citratus* against carbon tetrachloride-induced liver damage. Afr. J. Biochem. Res. 2020; 14(4):112-124.
39. Lawal M, Suleiman A, Matazu NU, Dawud FA, Mohammed A, UmarI A. Antidiabetic Activity of *Pistia strateotes* L. Aqueous Extractin Alloxan-induced Diabetic Rats. Trop J Nat Prod Res. 2019;3(3):91-94. doi.org/10.26538/tjnpr/v3i3.5.
40. Longe AO, Momoh JO**,** Asoro RI. Acute toxicity and hypoglycemic properties of ethanolic root extract of *Vernonia amygdalina* (bitter leaf) in alloxan-induced diabetic rats. Int.J.Curr.Res. 2017; 9(5):50132-50138.
41. Momoh JO, Manuwa AA, Oshin TT. Phytochemical screening, Gas chromatography: Mass spectrometry and antidiabetic properties of aqueous extract of ginger (*Zingiber officinale*) in Alloxan induced diabetic Wistar rats. J**.** pharmacogn**.** phytochem. 2022; 11(5):11-19.
42. Momoh JO**,** Ayinde FA, Awote OK, Adekunle OM, Obayomi AA. Antioxidant, inhibition of advanced glycation end-product formation and antimicrobial activities of *Ocimum gratissimum* (scent leaf) methanolic leaf extract against *Escherichia coli* and *Bacillus SPP*. J.Chem.Soc. Niger. 2023; 48(5): 800 – 819.
43. Bikanga R, Akué R, Nkounkou LC, Lebibi J, Louis-Clément OE, Ouamba JM. Phytochemical study and antioxidant

activities of *Terminalia catappa L*. and *Mitragyna ciliate* Aubrev and Pellegr medicinal plants of Gabon. J Med Plants Stud. 2019; 7(1): 33-38.
44. Muthulakshmi G, Neelanarayanan P. Evaluation of Antimicrobial Activities of *Terminalia catappa* Leaves' Extracts against Bacterial and Fungal Pathogens. Indian J. Nat. Sci. 2021; 11 (64).
45. Sowmya TN, Raveesha KA. Polyphenol-Rich Purified Bioactive Fraction Isolated from *Terminalia catappa* L.: UHPLC-MS/MS-Based Metabolite Identification and Evaluation of Their Antimicrobial Potential. Coatings. 2021;11: 1210. doi.org/10.3390/coatings11101210
46. Adeniyi MO, Momoh JO, Aderele OR. Experimental and Mathematical Model for the Antimalarial Activity of Metabolic Root Extract of *Azadirachtaindica* (Dongoyaro) in Mice Infected with *Plasmodium berghei NK65*, J. Adv. Math. Comput. Sci. 2020; 35(5): 68-82.
47. Theng KB, Korpenwar AN. Phytochemical Analysis of Ethanol Extract of *Ampelocissus Latifolia* (Roxb.) Planch Tuberous Root Using UV-Vis, FTIR, and GC-MS. Int J Pharm Sci Res. 2015; 6(9):3936-3942.
48. Siripi BR, Badal KM. Facile green synthesis of zinc oxide nanoparticles by *Eucalyptus globulus* and their photocatalytic and antioxidant activity. Adv.Powder Technol. 2017; 28. doi: 10.1016/j.apt.2016.11.026
49. Allyn OQ, Kusumawati E, Nugroho RA. Antimicrobial activity of *Terminalia catappa* brown leaf extracts against *Staphylococcus aureus* ATCC 25923 and *Pseudomonas aeruginosa* ATCC 27853. F1000Res. 2018;7:doi: 10.12688/f1000research.15998.1
50. Mbengui RD, Guessennd NK, Gervais MM, Julien KG, Constantin OO, Jean DN, Mireille D, Joseph AD. Phytochemical screening and study of comparative antibacterial activity of aqueous and alcoholic extracts of the leaves and barks of *Terminalia catappa* on multiresistant strains. J. Appl. Biosci. 2013; 66: 5040–5048.
51. Katiki LM, Gomes ACP, Barbieri AME, Pacheco PA, Rodrigues L, Veríssimo CJ, Gutmanis G, Piza AM, Louvandini H, Ferreira JFS. *Terminalia catappa*: Chemical composition, in vitro and in vivo effects on *Haemonchus contortus.* Vet Parasitol. 2017; 246: 118–123.
52. Okeke MI, Iroegbu CU, Eze EN, Okoli AS, Esimone CO. Evaluation of extracts the roots of *Landolphia owerrience* for antibacterial activity. J Ethanopharmacol. 2001;78: 119-127.
53. Momoh J, Olaleye ON, Odetunde SK. Antimicrobial and Antioxidant Properties of Aqueous Garlic (*Allium sativum*) Extract Against *Staphylococcus aureus* and *Pseudomonas aeruginosa*, Microbiol. Res. J. Int. 2016; 14(1): 1-11.
54. Gill AO, Holley RA. Disruption of *Escherichia coli, Listeria monocytogenes,* and *Lactobacillus sakei* cellular membranes by plant oil aromatics. Int.J.Food Microbiol. 2006;108: 1–9.
55. Mabasa XE, Mathomu LM, Madala NE, Musie EM, Sigidi MT. Molecular Spectroscopic (FTIR and UV-Vis) and Hyphenated Chromatographic (UHPLC-qTOF-MS) Analysis and In Vitro Bioactivities of the *Momordica balsamina* Leaf Extract. Biochem Res Int. 2021. doi: 10.1155/2021/2854217
56. Johnson M, Syed-Ali FM. Spectroscopic studies on *Pouzolzia wightii benn*. Int J Pharm Pharm Sci. 2018; 10 (3):124–132.
57. Krishnamoorthy K, Subramaniam P. Phytochemical Profiling of Leaf, Stem, and Tuber Parts of *Solena amplexicaulis* (Lam.) Gandhi Using GC-MS. Int. Sch. res. notices. 2014; doi.org/10.1155/2014/567409
58. Momoh JO, Olaleye ON. Evaluation of Secondary Metabolites Profiling of Ginger (*Zingiber officinale* Roscoe) Rhizome using GC-MS and Its Antibacterial Potential on *Staphylococcus aureus* and *Escherichia coli.* Microbiol. Res. J. Int. 2022; 32(7): 7-31.
59. Ahmad W, Kalra D. Green synthesis, characterization and antimicrobial activities of ZnO nanoparticles using *Euphorbia hirta* leaf extract. J. King Saud Univ. Sci. 2020;32: 2358-2364.
60. Suresh D, Nethravathi PC, Udayabhanu, Rajanaika H, Nagabhushana H, Sharma SC. Green synthesis of multifunctional zinc oxide (ZnO) nanoparticles using *Cassia fistula* plant extract and their photodegradative, antioxidant and antibacterial activities. Mater. Sci. Semicond. Process. 2015;31: 446-454.
61. Suresh D, Shobharani RM, Nethravathi PC, Pavan-Kumar MA, Nagabhushana H, Sharma SC. *Artocarpus gomezianus* aided green synthesis of ZnO nanoparticles: luminescence, photocatalytic and antioxidant properties. Spectrochim Acta Mol Biomol. Spectrosc. 2015;141: 128-134. doi: 10.1016/j.saa.2015.01.048
62. Pudukudy M, Yaakob Z. Facile synthesis of quasi-spherical ZnO nanoparticles with excellent photocatalytic activity. J. Cluster Sci. 2015; 26:1187-1201.
63. Sun JH, Dong SY, Feng JL, Yin XJ, Zhao XC. Enhanced Sunlight Photocatalytic Performance of Sn-Doped ZnO for Methylene Blue Degradation. J Mol Catal A Chem. 2011;335: 145-150. doi.org/10.1016/j.molcata.2010.11.026
64. Reddy AJ, Kokila MK, Nagabhushana H, Rao JL, Shivakumara C, Nagabhushana BM, Chakradhar RPS. Combustion synthesis, characterization, and Raman studies of ZnO nanopowders, Spectrochim. Acta Mol. Biomol. Spectrosc. 2011;81: 53-58.
65. Alharthi FA, Alghamdi AA, Alothman AA, Almarhoon ZM, Alsulaiman MF, Al-Zaqri N. Green synthesis of ZnO nanostructures using *Salvadora persica* leaf extract: applications for photocatalytic degradation of methylene blue dye. Crystals. 2020;10(6): doi.org/10.3390/cryst10060441
66. Rani KS, Mumtaz M, Priyank R, Chandran M. Phytochemical screening by FTIR spectroscopic analysis of methanol leaf extract of herb *Andrographis echioides*. J Ayu Herb Med. 2021; 7(4): 257-261.
67. Wetzel DL, Eilert AJ, Pietrzak LN, Miller SS, Sweat JA. Ultraspatially-resolved synchrotron infrared microspectroscopy of plant tissue in situ. Cell. Mol. Biol. 1998; 44 (1): 145-168.
68. Rad SS, Sani AM, Mohseni S. Biosynthesis, characterization and antimicrobial activities of zinc oxide nanoparticles from leaf extract of *Mentha pulegium (L.).* Microb. Pathog. 2019;131: 239– 245.
69. Zare M, Namratha K, Thakur MS, Byrappa K. Biocompatibility assessment and photocatalytic activity of bio-hydrothermal synthesis of ZnO nanoparticles by *Thymus vulgaris* leaf extract. Mater. Res. Bull. 2019; 109: 49–59.
70. Gupta R, Das N, Singh M. Fabrication and surface characterisation of c-ZnO loaded TTDMM dendrimer nanocomposites for biological applications. Appl. Surf. Sci. 2019;484:781–796.
71. Nagajyothi P, Sreekanth T, Tettey CO, Jun YI, Mook SH. Characterization, antibacterial, antioxidant, and cytotoxic activities of ZnO nanoparticles using *Coptidis Rhizoma*. Bioorg. Med. Chem. Lett. 2014; 24:4298–4303.
72. Sowndhararajan K, Joseph JM, Manian S. Antioxidant and free radical scavenging activities of Indian Acacias: *Acacia leucophloea* (Roxb.) Willd., *Acacia ferruginea* DC., *Acacia dealbata* Link. and *Acacia pennata* (L.) Willd. Int. J. Food Prop. 2013;16:1717–1729.
73. Awe FW, Faruruwa MD, Abba H. Green Synthesis, Characterization and Antibacterial Activity of Zinc Oxide and Titanium Dioxide Nanoparticles Using *Terminalia Catappa* and *Cymbopogon Citratus* Leaf Extract. Phys. Commun. 2021; 7(4): 563-572.
74. Muthuvel A, Jothibas M, Manoharan C. Effect of chemically synthesis compared to biosynthesized ZnO-NPs using *Solanum nigrum* leaf extract and their photocatalytic, antibacterial and in-vitro antioxidant activity. J. Environ. Chem. Eng. 2020;8: doi.org/10.1016/j.jece.2020.103705.
75. Brayner R, Ferrari-Iliou R, Brivois N, Djediat S, Benedetti MF, Fievet F. Toxicological impact studies based on *Escherichia*

ISSN 2616-0684 (Print)
ISSN 2616-0692 (Electronic)

coli bacteria in ultrafine ZnO nanoparticles colloidal medium. Nano Lett. 2006;6: 866–870.

76. Hameed ASH, Karthikeyan C, Kumar VS, Kumaresan S, Sasikumar S. Effect of Mg^{2+}, Ca^{2+}, Sr^{2+} and Ba^{2+} metal ions on the antifungal activity of ZnO nanoparticles tested against *Candida albicans*. Mater. Sci. Eng. C. 2015;52: 171–177.
77. Rahman A, Afzal R, Zulfiqar S, Alsafari IA, Khan MA, Agboola PO, Haider S, Warsi MF, Shakir I. Superior photodegradation and antibacterial activity of r-GO supported ternary nanocomposite of doped transition metal compounds. Ceram. Int. 2021;47:14569–14578.